Comparative histological study on the effect of tramadol abuse on the testis of juvenile and adult male albino mice

Amal T. Abou Elghait[1,2], Tarek. M. Mostafa[3], Fatma K. Gameaa[4], Gamal K. Mohammed[5], Fatma Y. Meligy[1], Manal M. Sayed[1]

[1]Department of Histology and Cell Biology, Faculty of Medicine, Assiut University, Assiut, [2]Department of Histology and Cell Biology, Sphinx University, New Assiut City, [3]Department of Anatomy and Embriology, Faculty of Medicine, Assiut University, Assiut, [4]Department of Histology and Cell Biology, Faculty of Medicine, Aswan University, Aswan, [5]Department of Histology and Cell Biology, Faculty of Veterinary Medicine, Assiut University, Assiut, Egypt

Abstract: As a synthetic analog of codeine, tramadol is often prescribed to treat mild to moderate pains. This study was designed to estimate and compare the histological effect of tramadol on testes of both juvenile and adult male albino mice. A total number of 40 healthy male albino mice were classified into two main groups as follows: group I (juvenile group, includes 20 mice aged three weeks) subdivided equally into group Ia (control group received isotonic saline) and group Ib (tramadol-treated group received 40 mg/kg/d tramadol orally for 30 days); group II (adult group, includes 20 mice aged two months) subdivided equally into group IIa (control group received isotonic saline) and group IIb (tramadol-treated group). Juvenile and adult tramadol-treated groups showed numerous testicular changes, including blood vessels congestion, widening of intercellular spaces, vacuolization in interstitial tissues, luminal germ cells exfoliation, and increased expression of caspase-3 that indicated cellular apoptosis. In the ultrastructural examination, spermatogenic cells degenerated with the frequent appearance of apoptotic cells. Sertoli cells showed vacuolations, large lipid droplets, and disrupted intercellular cell junctions. These observed testicular changes were markedly observed in the juvenile group. Testicular abnormalities and apoptotic changes can be caused by tramadol administration. These abnormalities are more common in juvenile mice.

Key words: Testis, Tramadol, Juvenile, Adult and apoptosis

Introduction

Tramadol is a synthetic opioid 4-phenylpiperidine codeine analog, it can bind with μ receptors, but its binding ability with δ- and κ-opioid receptors is low [1]. Tramadol is recommended to treat pain with different degrees of severity [2].

Corresponding author:
Fatma Y. Meligy
Department of Histology and Cell Biology, Faculty of Medicine, Assiut University, Assiut 71516, Egypt
E-mail: fmeligy@aun.edu.eg

As various tramadol formulations are available, it is increasingly prescribed worldwide as an alternative for high-affinity opioid medication in acute and chronic pain treatment (especially acute perioperative pain) [3]. Routes of tramadol administration are oral, rectal, or parenteral (intravenous, intramuscular, and subcutaneous) routes. Dose titration should be followed according to pain intensity and individual response [4] Tramadol's efficacy to overcome moderate to extreme postoperative pain has been proven in both day surgery and hospitalized patients. Moreover, it has been demonstrated that using tramadol (orally or parentally) is as effective as a painkiller during perioperative care [5].

Although it is a good painkiller, poisoning can be devel-

oped due to tramadol abuse that happens in overdosage, use for an extended period, or interaction with other drugs [6]. Furthermore, severe neurological toxicity involving seizures, respiratory failure, coma, and mild tachycardia with hypertension may result from tramadol overdosage [7]. In addition, many authors indicated that opioids addiction or their consumption for an extended period, such as tramadol and morphine, can cause a lot of adverse effects such as decreasing in sexual activity, dropping in the production of follicle-stimulating hormone (FSH), and testosterone, and hypothalamic-pituitary function abnormalities [8, 9]. It was proved that low-safe and controlled doses of tramadol could be an effective treatment for early or premature ejaculation in mild and severe cases [10].

Although many scientific works studied the side effects of tramadol administration, the impact of tramadol on testicular tissues from a histopathological view needs more investigation. So, this work was designed to investigate histopathological and morphological testicular changes that occur with tramadol administration and compare these testicular changes between adult and juvenile male mice.

Materials and Methods

Drugs and chemicals

Tramadol hydrochloride (125 mg tablets) was supplied from MINA Pharm, 10th of Ramadan City, Cairo Governorate, Egypt, by official request to the dean of the Faculty of Medicine through the pharmacy of Assiut University Hospital.

Animals

From Animal House of Assiut University, a total number of 40 healthy male albino mice were purchased. Animals were maintained under controlled conditions of humidity and temperature. Light:dark cycle was carefully arranged. Standard food and fresh, clean water were supplied *ad libitum*. The procedures of the experiment were carried out according to the internationally accepted guidelines for the Care and Use of Laboratory Animals and were approved by the Ethics Committee at the Faculty of Medicine, Aswan University, Aswan, Egypt (123-4-17).

Experimental design

Forty mice were divided equally into two major groups, and each one was subdivided into two other groups:

Group I (juvenile group): twenty mice weighting 10–15 g, aged three weeks, were subdivided into:

Group Ia: control group (n=10) received isotonic saline.

Group Ib: tramadol treated group (n=10) received 40 mg/kg/d tramadol, as tablets were smashed and dissolved in normal physiological saline (0.9% orally one time/d for 30 days).

Group II (adult group): twenty mice weighting 25–30 g, aged two months, were subdivided into:

Group IIa: control group (n=10) received isotonic saline.

Group IIb: tramadol treated group: (n=10) received 40 mg/kg/d tramadol, tablets were treated as in group Ib.

Histological examination

Light microscope examination

Testis specimens were collected from all groups, fixed in bouin for 16 to 18 hours, washed with 70% alcohol, dehydrated through ascending graded alcohols and embedded in paraffin, microtome sectioned at 5-μm thickness [11], and stained with the following stains:

1. H&E stain: for general histological examination.

2. Masson's trichrome: for collagen fibers demonstration.

All staining methods were done following the steps described by Bancroft and Layton [12].

Electron microscope examination

Testis specimens were immersed in glutaraldehyde (4%) in cacodylate buffer (pH 7.4) for 24 hours and postfixed for 2 hours in osmium tetroxide (1%) in phosphate buffer solution (PBS). Tissues were rinsed with the same buffer, dehydrated with alcohol, cleared with propylene oxide, and embedded in Epon-812 substitute. Semi-thin sections (0.5–1 μm) were cut with glass knives on the ultratome, and toluidine blue (1%, pH 7.3) was used for staining to be examined on a light microscope. Ultrathin sections (50–80 nm) were cut on a Reichert ultratome, placed on copper grids, and contrasted with uranyl acetate and lead citrate. A transmission electron microscope (Jeol E.M.-100 CX11; Japanese Electron Optics Laboratory Co., Ltd, Tokyo, Japan) was used to examine these sections. Photographing was done at 80 kV in Assiut Electron Microscopic Unit, Assiut University [13].

Immunohistochemical staining

Testis paraffin sections with rabbit anti-mouse caspase-3 polyclonal antibody 1:100 (Chongqing Biospes Co., Ltd.,

Chongqing, China) were used to demonstrate apoptotic cells. According to O'Callaghan and Jensen [14], the avidin-Biotin peroxidase technique was used. Sections were incubated with primary antibodies diluted; at 1:100 in PBS and left overnight at room temperature. After that, they were stained with an avidin-biotin-peroxidase system using diaminobenzidine as the chromogen (horseradish peroxidase [HRP]; rabbit/mouse/goat [DAB+] code no. K0679, DakoCytomation; Dako, Glostrup, Denmark) in conformity with the staining procedure instruction included in Dako LSAB+ System-HRP (Dako). Sections were washed in distilled water and counter-stained with hematoxylin.

Morphometric studies

Morphometric studies were done using a Java-based open-source image processing package, ImageJ (National Institutes of Health, Bethesda, MD, USA). The required parameters were measured in five fields/five non-overlapped sections from three mice from each group. The measured parameters were: the thickness of the capsule, the thickness of the germinal epithelium, the number of positive (+) caspase immune-stained cells and number of distorted seminiferous
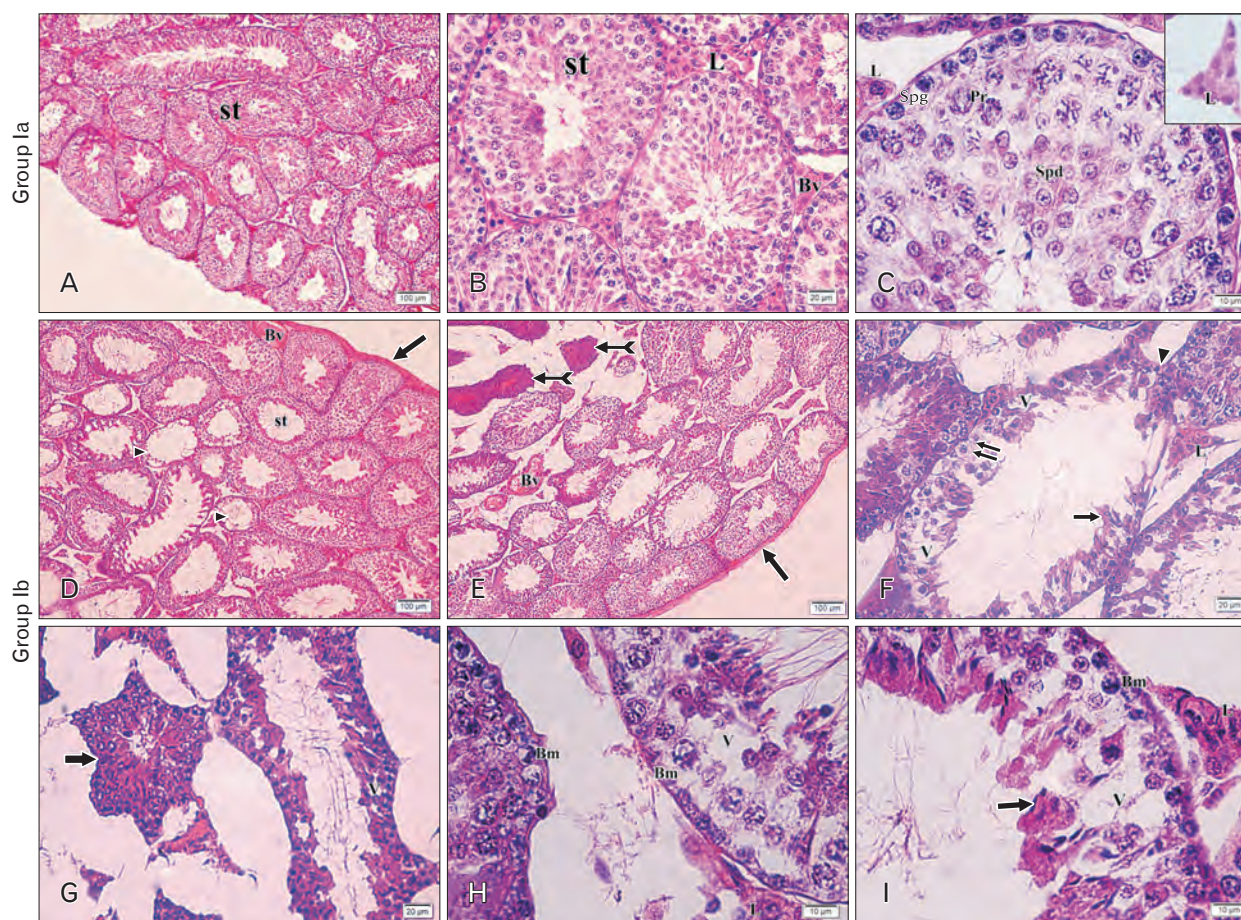
Fig. 1. Photomicrographs of a sections of the testis from mice stained by H&E. Group Ia (A–C): (A) Normal closely packed seminiferous tubules (st) with normal contour (×100). (B) The interstitial cell of Leydig (L) are present surrounding blood vessels (Bv) (×400). (C) A magnified photomicrograph showing spermatogonia (Spg), primary spermatocytes (Pr), and rounded early spermatids (Spd). Inset shows a group of Leydig cells with rounded nuclei and acidophilic cytoplasm (×1,000). Group Ib (D–I): (D, E) Group of seminiferous tubules (st) surrounded by a connective tissue capsule (arrows), some tubules show depletion of spermatogenic cells (arrowheads). Other tubules appeared shrunken with obliteration of the lumen and increase acidophilia (tailed arrows). The blood vessels appear congested (Bv) (×100). (F, G) Disorganized germinal epithelium (arrows), focal vacuoles between the destructed cells (V), and swelling in some cells (double arrow) can be observed. Group of interstitial cells of Leydig (L) with dark irregular nuclei and amalgamated highly acidophilic cytoplasm are also seen. Notice fusion between some tubules (arrowhead) (×400). (H, I) Magnified photomicrographs showing a thick irregular basement membrane (Bm), disorientation of late spermatids (arrow), and multiple focal vacuoles (V) between cells. The interstitial cells of Leydig (L) appear with irregular dense nuclei and highly acidophilic cytoplasm (×1,000).

tubules. Images of stained sections captured at 400× magnification were used for the thickness of the capsule, the thickness of the germinal epithelium and the number of positive (+) caspase immune-stained while for counting number of distorted seminiferous tubules, we used 100× magnification

Statistical analysis

Data were expressed as mean±standard error of the mean. Statistical analysis was performed by multiple *t*-tests, one-way and two-way repeated-measures ANOVA, followed by post hoc Tukey's test when appropriate. All statistical tests were directed using GraphPad Prism 7 software (GraphPad Software Inc., San Diego, CA, USA). The difference among groups was considered significant at *P*<0.05.

Results

Light microscopy results

Hematoxylin and eosin-stained sections results

Tramadol administration (40 mg/kg body weight [BW]/d for 30 days) showed morphological changes in the seminiferous tubules and interstitial tissue in both juvenile and adult groups. The changes were more severe in the juvenile group (Ib) than in the adult group (IIb). Our results showed that group Ia (juvenile control group) showed that the transverse sections in seminiferous tubules appeared regular rounded or oval, separated by interstitial connective tissue and covered by a connective tissue capsule (Fig. 1A, B). The seminiferous tubules were lined by germinal epithelium and surrounded by a basement membrane and a layer of peritubular myoid cells which are flat cells with flat nuclei. The germinal epithelium was formed of spermatogenic cells and supporting Sertoli cells. The spermatogenic cells included spermatogonia, primary spermatocytes, rounded spermatids, and sperms. In between tubules, the interstitial cells of Leydig with rounded nuclei and acidophilic cytoplasm were noticed surrounding the blood capillaries (Fig. 1A, C).

The spermatogonia were arranged as one raw next to the basement membrane with oval nuclei. The primary spermatocytes were represented in the next row of germinal epithelium cells, usually two or three layers. They were the largest of the whole series, having rounded large nuclei with different stages of meiotic division (Fig. 1C). The rounded or early spermatids revealed rounded nuclei and presented in multiple rows (Fig. 1C).

In group Ib (juvenile tramadol-treated group), sections-stained with H&E stain showed severe distortion in most seminiferous tubules; they were irregular in shape, widely separated, and degenerated. The thickness of the germinal epithelium was reduced significantly compared to the control group with irregular empty spaces. Few or no sperms were found. However, few tubules appeared nearly similar to the control group (Fig. 1D, E). Shrinkage with increased acidophilia was observed in some tubules (Fig. 1D, F), while others were severely shrunken up to appear star-shaped (Fig. 1G). In addition, fusion occurred between some tubules with swelling of some cells and irregular vacuoles or empty spaces between cells (Fig. 1F). Congestion of blood vessels was noticed (Fig. 1D, E).

In some sections, exfoliation, vacuolation, and pyknosis of germ cells were prominent features (Fig. 1G–I). The basement membrane showed irregularity with increased thickness (Fig. 1F). The interstitium showed transudation, increased interstitial cellular mass, and congested blood vessels (Fig. 1D, E). Leydig cells were seen with darkly stained nuclei and deeply acidophilic cytoplasm (Fig. 1H, I).

Group IIa (adult control group), the same as group Ia, rounded or oval regular seminiferous tubules enclosed by a connective tissue capsule and surrounded by interstitial connective tissue were detected (Fig. 2A). The germinal epithelium was seen lining the tubules and basement membrane surrounding them. The germinal epithelium was formed of spermatogenic cells (spermatogonia, primary spermatocytes, rounded spermatids, and sperms) and supporting Sertoli cells (Fig. 2A, B). Interstitial cells with round nuclei and acidophilic cytoplasm were observed (Fig. 2B).

One raw next to the basement membrane, spermatogonia with ovoid nuclei were arranged. Primary spermatocytes were found in the following raw germinal epithelium cells (usually two or three layers). They were the largest of the whole series, having rounded large nuclei with different stages of meiotic division (Fig. 2B). The rounded spermatids revealed rounded nuclei and presented in multiple rows. At the same time, elongated spermatids had condensed elongated nuclei and tails that protrude to the lumen (Fig. 2A). The Sertoli cells had large pale nuclei with prominent nucleoli resting on the basement membrane (Fig. 2A). Large Leydig cells were found in the interstitium with round nuclei and light acidophilic cytoplasm adjacent to a blood vessel (Fig. 2A).

Group IIb (adult tramadol-treated group), sections stained

with H&E stain showed distortion in most seminiferous tubules. They were widely separated with irregularity. Furthermore, a thick, irregular testicular capsule was observed (Fig. 2C). Few numbers of tubules were more or less the same as in the control group (Fig. 2C). Exfoliation of dense acidophilic germ cells with vacuolation, increased mitotic activity, and irregularity of basement membrane were detected (Fig. 2C–E). Transudation, congestion of blood vessels, and increased interstitial cellular mass were found in the interstitium. Deeply acidophilic cytoplasm and darkly stained nuclei were detected in Leydig cells (Fig. 2E, F).

The thickness of germinal epithelium decreased significantly in Tramadol-treated juvenile group when compared with the control juvenile group (*P*<0.001). The tramadol-treated adult group showed a significantly reduced thickness of germinal epithelium versus the control adult group (*P*<0.001). The thickness of germinal epithelium was reduced considerably in tramadol treated juveniles than Tramadol treated adult groups (*P*<0.001; Fig. 3).

The number of distorted tubules was increased signifi-
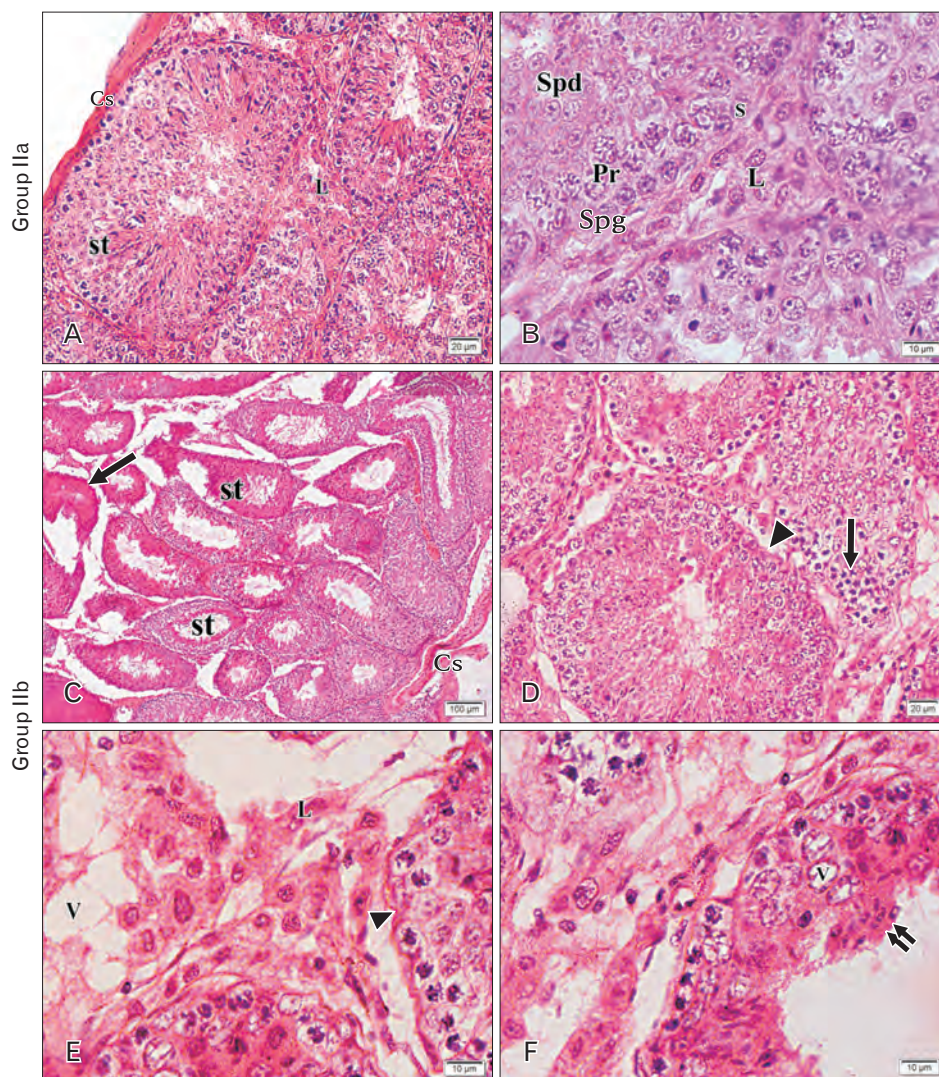
Fig. 2. Photomicrographs of a sections of the testis from mice from the stained by H&E. Group IIa (A, B): (A) Normal regular appearance of seminiferous tubules (st) surrounded by a regular capsule (Cs) (×400). (B) A magnified photomicrograph of the previous section showing spermatogenic cells formed of spermatogonia (Spg), primary spermatocytes (Pr), and early spermatids (Spd). Sertoli cell (S) and Leydig cells (L) can be seen (×1,000). Group IIb (C–F): (C) Irregular deformed highly acidophilic seminiferous tubules (st) some tubules have no lumen (arrow). They are surrounded by a thick irregular capsule (Cs) (×100). (D) Increased mitotic activity (arrow). Irregular basement membrane (arrowhead) can be noticed (×400). (E, F) Magnified photomicrographs showing vacuolation (V), disorganized germinal epithelium (double arrow), thick irregular basement membrane (arrowhead), and increased interstitial Leydig cell mass (L) (×1,000).
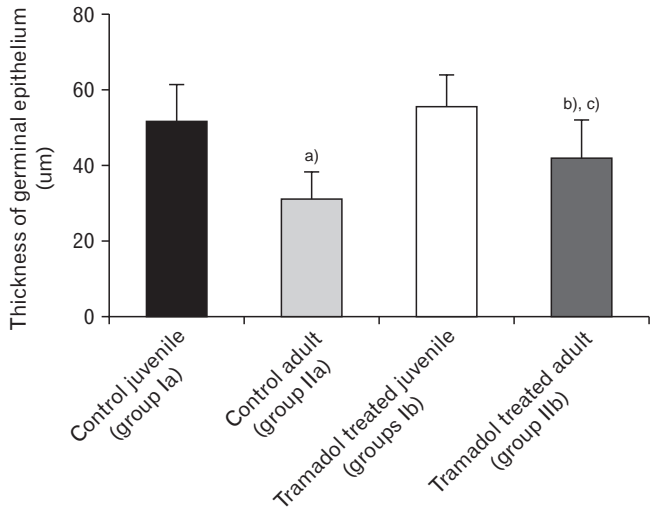
Fig. 3. The thickness of germinal epithelium was decreased significantly in Tramadol treated juvenile group when compared with the control juvenile group ([a]$P<0.001$). Tramadol treated adult group showed a significantly decreased thickness of germinal epithelium versus the control adult group ([b]$P<0.001$). The thickness of germinal epithelium was significantly reduced in Tramadol treated juvenile than Tramadol treated adult groups ([c]$P<0.001$).
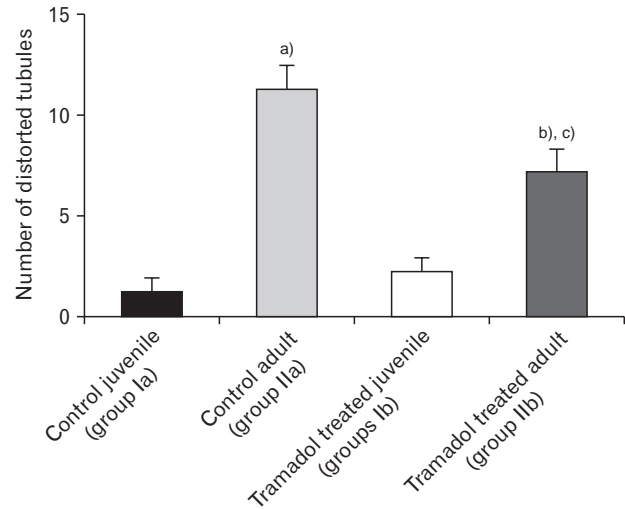
Fig. 4. The number of distorted tubules was increased significantly in Tramadol treated juvenile group in comparison with the control juvenile group ([a]$P<0.001$). Tramadol treated adult group has a significantly increased number of distorted tubules than the control adult group ([b]$P<0.001$). Tramadol treated juvenile group showed a significantly higher number of distorted tubules than the Tramadol treated adult group ([c]$P<0.001$).

Fig. 5. (A–D) Photomicrographs of a sections of the testis from mice stained by Masson trichrome (×400). (A) In group Ia, normal distribution of collagen fibers in the testicular capsule (Cs) and basement membrane of seminiferous tubules (arrow). (B) In group Ib, excess collagen fibers in the testicular capsule (Cs) and around blood vessels (Bv). (C) In group IIa, normal distribution of collagen fibers in testicular capsule (Cs) and basement membrane of seminiferous tubules (arrow). (D) In group IIb, dense collagen fibers deposition in the capsule (Cs), and in the basement membrane of the seminiferous tubules (arrow). Note the severely congested blood vessel (Bv). (E) Graphical representation of the mean of the Seminiferous tubule capsule thickness. Data are expressed as mean±standard error of the mean. The capsule thickness was increased significantly in Tramadol treated juvenile group in comparison with the control juvenile group ([a]$P<0.001$). Tramadol treated adult group has a significantly increased capsule thickness versus the control adult group ([b]$P<0.05$). An insignificant difference was obtained between the Tramadol-treated juvenile and Tramadol-treated adult groups.

cantly in Tramadol treated juvenile group in comparison with the control juvenile group (*P*<0.001). Tramadol treated adult group has a significantly increased number of distorted tubules than the control adult group (*P*<0.001). Tramadol treated juvenile group showed a significantly higher number of distorted tubules than the Tramadol treated adult group (*P*<0.001; Fig. 4).
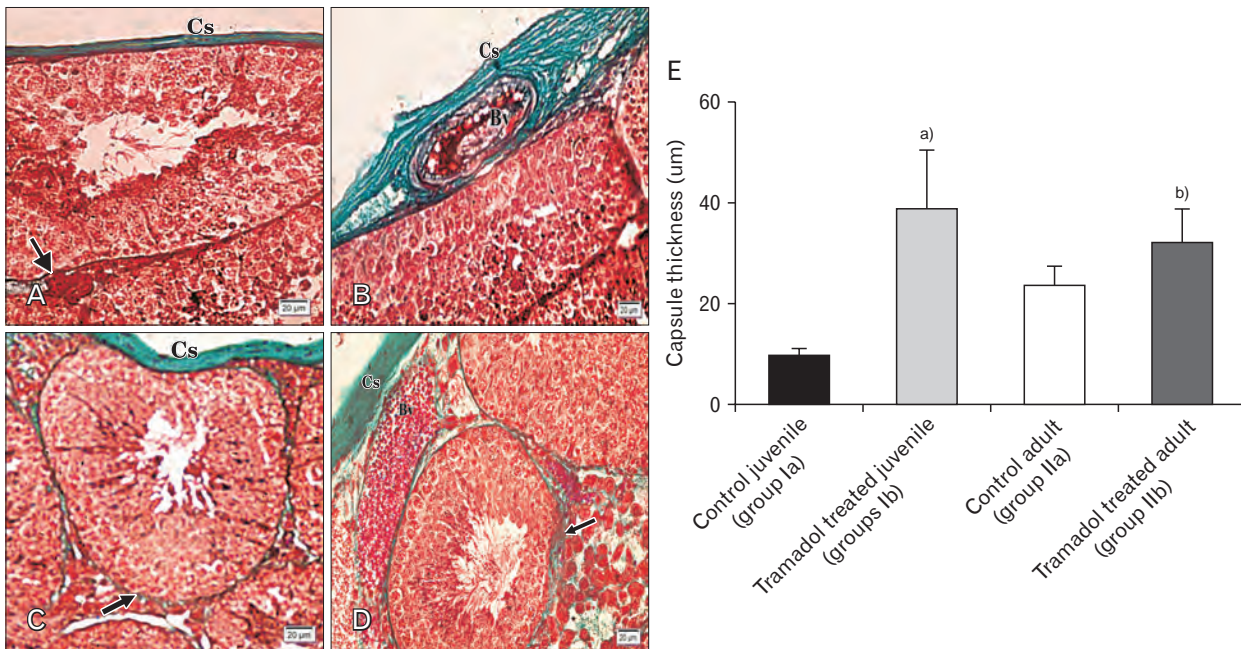
Masson's trichrome stained sections

In group Ia, regular distribution of collagen fibers in the capsule with few depositions around blood vessels was detected during Masson trichrome stained sections examina-

tion (Fig. 5A). Group Ib, most of the seminiferous tubules showed dense deposition of the collagen fibers, causing thickening in the capsule and around blood vessels, as well as the basement membrane (Fig. 5B). Group IIa, in the capsule, collagen fibers showed normal distribution, while around blood vessels and basement membranes, few depositions of collagen fibers were found (Fig. 5C). Group IIb, collagen fibers showed dense deposition surrounding basements membrane, blood vessels, and in the capsule (Fig. 5D).

The capsule thickness was increased significantly in Tramadol treated juvenile group in comparison with the control juvenile group (*P*<0.001). Tramadol treated adult group has
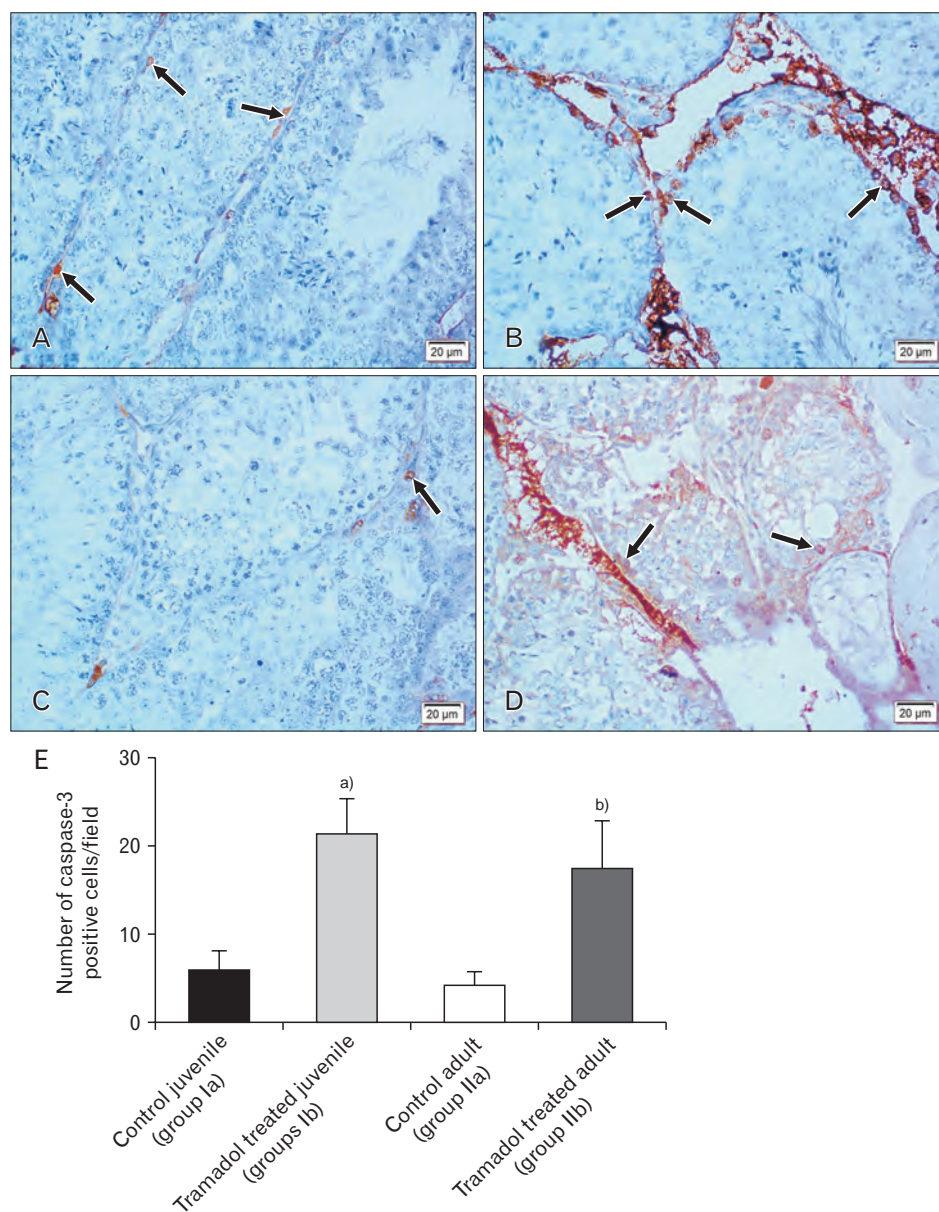

Fig. 6. (A–D) Photomicrographs of a sections of the testis from mice stained by caspase-3 (×400). (A, C) Few positive staining cells in control groups Ia and IIa respectively. (B, D) Increased positive cells in both tramadol-treated groups Ib and IIb. (E) Graphical representation of the mean of the number of positive cells. Data are expressed as mean±standard error of the mean (n=6). The tramadol-treated juvenile group showed significantly higher caspase-3 positive cells than the control juvenile group ([a]*P*<0.001). Also, the Tramadol-treated adult group has a significantly increased number of caspase-3 positive cells than the control adult group ([b]*P*<0.001). An insignificant difference was obtained between the Tramadol-treated juvenile and Tramadol-treated adult groups. The arrows refer to the positive immunostained cells

a significantly increased capsule thickness versus the control adult group (*P*<0.05). An insignificant difference was obtained between the Tramadol-treated juvenile and Tramadol-treated adult groups (Fig. 6E).

Semithin section stained with toluidine blue

In group Ia, the seminiferous tubules appeared separated by interstitial connective tissue. A thin regular basement membrane surrounded them with myoid cells which were flat cells with flat nuclei. Spermatogonia had ovoid-shaped nuclei resting on the basement membrane. Primary spermatocytes had rounded large central nuclei in different stages of meiosis. Early or rounded spermatids showed acrosomal caps covering the rounded nuclei. The Sertoli cells were characterized mainly by their vesicular nuclei and resting on the basement membrane between spermatogenic cells. Leydig cells with spherical vesicular nuclei were seen between seminiferous tubules (Fig. 7A). Group Ib semithin sections revealed distorted irregular seminiferous tubules

separated by wide interstitial spaces with a marked increase in interstitial cell mass, and deeply stained nuclei of interstitial cells were frequently observed in comparison to control group with hazard arranged germ cells with multiple irregular empty spaces. Some Sertoli cells are detached from the basement membrane with depletion of sperms (Fig. 7B, C).

In group IIa, rounded and oval seminiferous tubules were separated by interstitial connective tissue. A thin regular basement membrane surrounded each seminiferous tubule with myoid cells, which appeared flat. Spermatogonia appeared with ovoid-shaped nuclei resting on the basement membrane. Primary spermatocytes had rounded large central nuclei in different stages of meiotic division. Early spermatids showed acrosomal caps covering the rounded nuclei. Sertoli cells appeared with vesicular nuclei, resting on the basement membrane in between spermatogenic cells. Sperms were seen in the lumen attached to Sertoli cells. Leydig cells with spherical vesicular nuclei and vacuolated cytoplasm were wedged in between seminiferous tubules
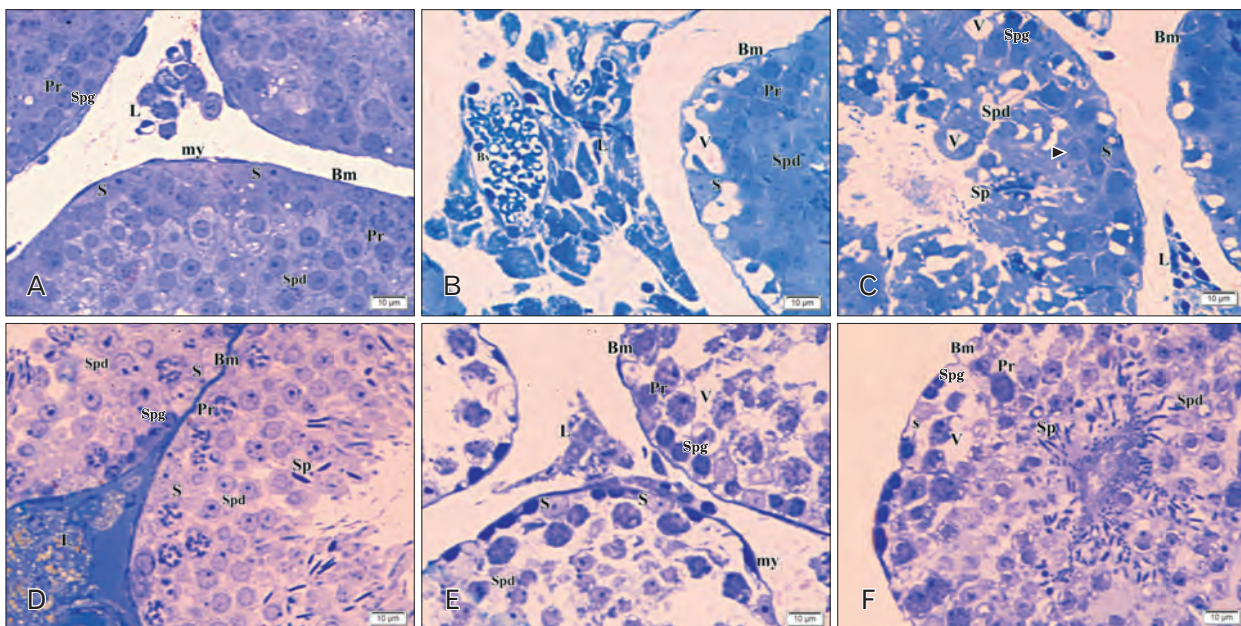

Fig. 7. Photomicrographs of a sections of the testis from mice stained by Toluidine blue (×1,000). (A) In group Ia, normal organization of spermatogenic cells. Spermatogonia (Spg), primary spermatocytes (Pr), and spermatids (Spd). Sertoli cell (S) appears with a regular vesicular nucleus and prominent nucleolus. Regular basement membrane (Bm) and myoid cell (my) are noticed. The interstitial cells of Leydig (L) are observed. (B, C) In group Ib, seminiferous tubules with hazard arranged germ cells with dense nuclei and multiple vacuolations (V). Some of Sertoli cells are detached from the basement membrane (head arrow). The basement membrane (Bm) is irregular. Increased cellularity of interstitial tissue (L) surrounding congested blood vessel (Bv). Sperm (Sp) could be seen. (D) Group IIa, seminiferous tubules are surrounded by a regular basement membrane (Bm) and have the normal organization of spermatogenic cells. Spermatogonia (Spg), primary spermatocytes (Pr), normal spermatids (Spd) with normal sperm (Sp) morphology and orientation. Sertoli cell (S) with a regular vesicular nucleus and prominent nucleolus. The interstitial cells of Leydig (L) can be observed. (E, F) In group IIb, spermatogonia (Spg) with dense nuclei, multiple vacuolations (V), darkly stained primary spermatocytes (Pr), degenerated irregular spermatids (Spd). Sertoli cells (S) show irregular nuclei. Myoid cells (my) with dense nuclei can be seen. Note the irregular basement membrane (Bm). The interstitial cells of Leydig (L) can be observed. Sperm (Sp) could be seen.

(Fig. 7D). In group IIb, the seminiferous tubules appeared distorted, irregular, and separated by wide interstitial spaces compared to the control group. Some tubules showed hazard arranged germ cells with multiple irregular empty spaces, and irregular shrunken Sertoli cells with irregular basement membranes (Fig. 7B, C).

To explore whether treatment with tramadol can induce apoptosis, we evaluated the expression of the apoptotic parameter caspase-3 in testicular tissues using the immunohistochemistry technique.

Group Ia: Immunostaining with caspase-3 showed scattered distribution of weakly positive apoptotic cells, especially in spermatogonia (Fig. 6A). In group Ib a significantly increased frequency of strongly positive apoptotic cells in spermatogonia and interstitial cells of Leydig (Fig. 6B). In group IIa, few weak positive caspase-3 immunostained cells were observed (Fig. 6C). Group IIb, significantly increased the frequency of moderately positive apoptotic cells in nearly all spermatogenic cells and interstitial cells of Leydig (Fig.

6D).

The tramadol-treated juvenile group showed significantly higher caspase-3 positive cells than the control juvenile group ($P<0.001$). Also, the Tramadol-treated adult group has a significantly increased number of caspase-3 positive cells than the control adult group ($P<0.001$). An insignificant difference was obtained between the Tramadol-treated juvenile and Tramadol-treated adult groups (Fig. 6E).

Electron microscopy results

Group Ia

Electron microscopic examination for this control group showed the presence of a regular thin basement membrane around the seminiferous tubule with myoid cells (with flat nuclei), while spermatogenic cells and Sertoli cells were lining them (Fig. 8A). Settling on the basement membrane, Sertoli cells were found with large basally located nuclei and prominent nucleoli with the fine distribution of granular
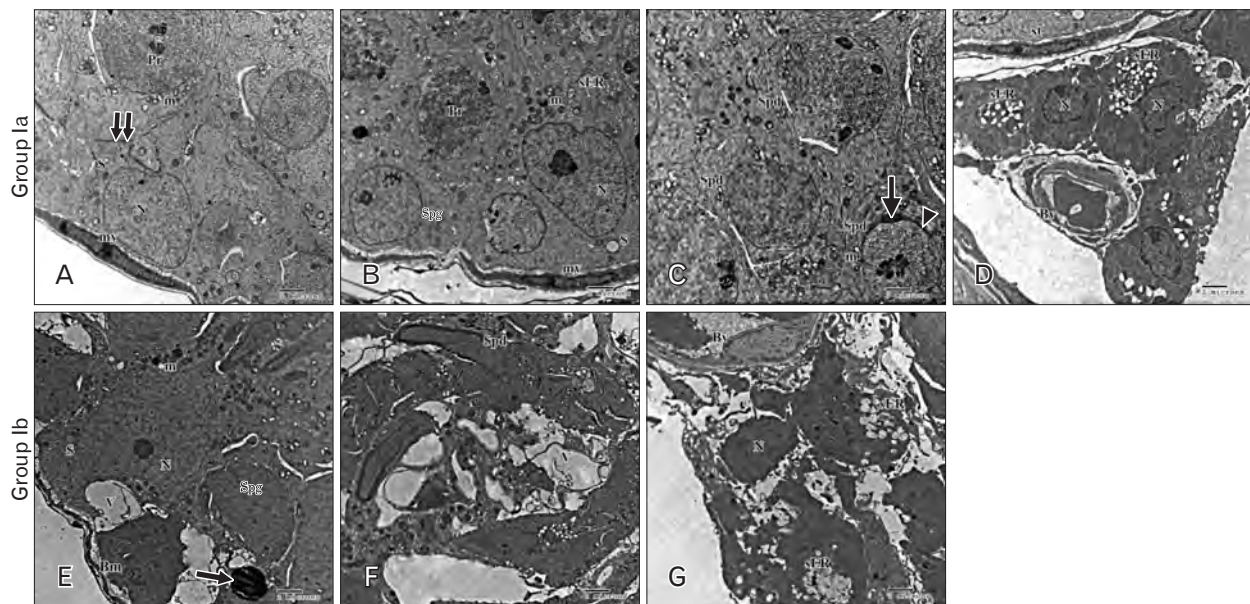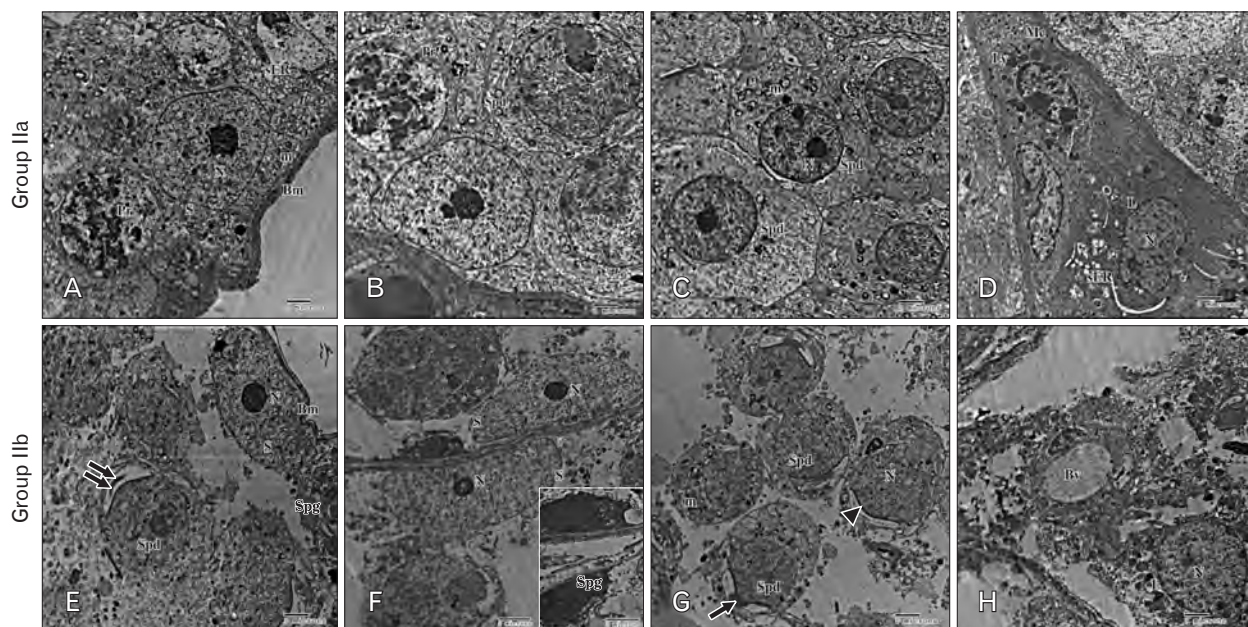

Fig. 8. Transmission electron microscopy of sections of the testis of mice (×3,600). A–D represent group Ia and E–G for group Ib. (A, B) The seminiferous tubules are surrounded by a thin regular basement membrane and the myoid cells (my) appear with their flattened nuclei. Sertoli cell (S) has a regular euchromatic nucleus (N), central nucleolus, smooth endoplasmic reticulum (sER), and mitochondria (m). Spermatogonia (Spg) is rested on the basement membrane. Primary spermatocyte (Pr) with a large rounded nucleus and finely dispersed chromatin and peripherally arranged mitochondria. An intact intercellular junction (double arrow) is observed. (C) Rounded spermatids (Spd) have spherical euchromatic nuclei and a cytoplasm showing peripherally arranged mitochondria (m). Acrosomal dense granule (arrow) and acrosomal cap (arrowhead) spread over the nucleus pole can be observed. (D) Group of Leydig cells with rounded euchromatic nuclei and cytoplasm rich in smooth endoplasmic reticulum (sER) surrounding blood vessel (Bv). Seminiferous tubules (st) and nucleus (N) could be seen. (E) Sertoli cell (S) with a large nucleus (N) and a prominent nucleolus, vacuolated cytoplasm (V), and small mitochondria (m). Large lipid droplet (arrow), irregular electron-dense spermatogonia (Spg) with vacuolated cytoplasm can be noticed (V). (F) Disorientation of elongated spermatids (Spd) and a group of degenerated cells with multiple empty spaces (V) are present. (G) Group of electron-dense Leydig cells with irregular dense nuclei (N) and dilated smooth endoplasmic reticulum (sER) can be seen around a blood vessel (Bv).

chromatin. Their cytoplasm had smooth endoplasmic reticulum, several mitochondria, and lysosomes (Fig. 8A, B). Spermatogonia with round nuclei were found in the basal compartment (Fig. 8B), and intercellular junctions were intact (Fig. 8A). Primary spermatocytes showed large rounded nuclei with finely granular chromatin and clumps of heterochromatin, and their cytoplasm was rich in mitochondria (Fig. 8A). Rounded spermatids were seen with spherical nuclei and finely granulated chromatin distribution. The nuclear membrane was thickened in a particular area and covered by the acrosomal cap and vesicle. The acrosomal cap was seen over one pole of the nucleus. The cytoplasm contained characteristic peripherally situated mitochondria with clear matrix and dilated cristae (Fig. 8C). Clumps of Leydig cells were present in the interstitium and had round or oval euchromatic nuclei, with several mitochondria and smooth endoplasmic reticulum in the cytoplasm (Fig. 8D).

Group Ib

The germinal epithelium of most seminiferous tubules, showed cellular loss, severe distortion, and extreme vacuolation in the cytoplasm. The intercellular junctions were not observed. A thickened irregular basement membrane surrounded them with myoid cells (Fig. 8E, F).

In some tubules, Sertoli cells showed irregular nuclei with the cytoplasm appearing rarified with empty spaces, devoid of organelles apart from abnormally shaped mitochondria. The spermatogenic cells appeared dark with various signs of degeneration varying from irregular dark nuclei and rarified cytoplasm. Degenerated elongated spermatids with irregular elongated acrosomal caps and irregularly arranged mitochondria were detected. The interstitial cells of Leydig appeared with rounded electron-dense nuclei, dilated smooth endoplasmic reticulum, and disrupted cell membrane (Fig. 8E–G).

Fig. 9. Transmission electron microscopy of sections in the testis of mice (×3,600). A–D photos represent group IIa while E–H for group IIb. (A, B) Sertoli cells (S) with large rounded euchromatic nuclei (N), central nucleoli and finely dispersed chromatin, smooth endoplasmic reticulum (sER), and mitochondria (m). A primary spermatocyte (Pr) with a rounded nucleus is present. Round spermatid (Spd) with a rounded regular nucleus. The cells rest on a basement membrane (Bm). (C) Rounded spermatids (Spd) have spherical euchromatic nuclei (N) and cytoplasm rich in small-sized mitochondria (m). (D) The interstitial tissue containing Leydig cell (L) with oval to rounded euchromatic nuclei (N) and cytoplasm rich in smooth endoplasmic reticulum (sER). A macrophage (Mc) with an oval nucleus and cytoplasm engorged with lysosomes (Ly) can be noticed. (E, F) Sertoli cell (S) with large vesicular nuclei (N) and prominent nucleoli resting on an irregular basement membrane (Bm). The cytoplasm appears degenerated and rarified. Dark spermatogonia (Spg) and irregular spermatid (Spd) with capping deformity (double arrow) are observed. The inset shows spermatogonia (Spg) with electron-dense cytoplasm and an ill-defined nucleus. (G) Spermatids (Spd) appear with degenerated cytoplasm, irregular nuclei (N), peripherally arranged mitochondria (m), with capping deformity (arrowhead) and acrosomal granule (arrow). (H) Leydig cell (L) with rounded nucleus (N) and irregular degenerated cytoplasm. The interstitial blood vessel can be noticed (Bv).

Group IIa

The seminiferous tubules of the control adult testis were lined by spermatogenic cells and the supporting Sertoli cells. Sertoli cells were rested on the basement membrane, and had large basally located nuclei with prominent central nucleoli and finely granular chromatin distribution. The Sertoli cell cytoplasm was studied with numerous mitochondria and smooth endoplasmic reticulum. Primary spermatocytes showed large rounded nuclei with finely granular chromatin and clumps of heterochromatin (Fig. 9A, B). The rounded spermatids were seen with spherical nuclei with finely granular chromatin distribution. The cytoplasm contained characteristic peripherally situated mitochondria (Fig. 9C). The interstitium showed Leydig cells with oval to rounded euchromatic nuclei. The cytoplasm revealed numerous smooth endoplasmic reticulum (Fig. 9D).

Group IIb

In this group, most of the seminiferous tubules showed a predominance of Sertoli cells with loss of most spermatogenic cells. The spermatogenic epithelium was severely distorted with excessive cytoplasmic vacuolation and cellular loss. An irregular basement membrane surrounds them with contracted dark myoid cells. Sertoli cells showed small nuclei in some tubules, and the cytoplasm was rarified with empty spaces (Fig. 9E). The spermatogenic cells showed various signs of degeneration with irregular nuclei (Fig. 9F).

Degenerated rounded spermatids with dark nuclei and abnormal chromatin distribution (Fig. 9F, G). A cluster of electron-dense Leydig cells was present with dark nuclei, and dilated smooth endoplasmic reticulum and lysosomes could be observed (Fig. 9H).

Discussion

Because of its high availability with low price, tramadol is relatively popular among Egyptian youth for alleged uses in premature ejaculation treatment and its ability to treat different pain degrees (moderate to severe, acute, and chronic pain) [10, 15, 16].

The objective of this study was to investigate light and electron microscopic changes observed in seminiferous tubules and interstitial cells after tramadol administration in juvenile and adult mice.

Light microscopic examination of control groups (Ia and IIa) revealed a typical histological picture of seminiferous tu-

bules; they appeared regularly with normal spermatogenesis and interstitial tissue. In addition, spermatogenic cells appeared normal and regularly organized. Moreover, the germinal epithelium thickness was greater than treated groups, as indicated by morphometrical studies. These results were in accordance with several studies that reported normal spermatogenesis and normal intertubular tissue [17, 18].

Tramadol administration (40 mg/kg BW/d for 30 days) showed structural changes in the seminiferous tubules and interstitial tissue in both juvenile and adult groups. These changes were more severe and prominent in the juvenile group (Ib) than in the adult group (IIb) that received tramadol for the same duration. In some animals, seminiferous tubules were largely separated from each other with loss of their normal contour. Some tubules' depletion of spermatogenic cells with excessive vacuolations was observed, while shrinkage of tubules, lumen obliteration, and increased acidophilia were found in other tubules. The number of distorted tubules was higher in treated group compared to control, with more increase in juvenile group. These findings were in line with the results obtained by Abdellatief et al. (2015) [17], they investigated the testicular changes in rats affected by long-term tramadol administration and attributed this to the deposition of homogenous hyaline acidophilic Periodic acid-Schiff-positive material. In contrast, Salama et al. (2003) [19] explained the wide separation between the seminiferous tubules. It may be related to the degeneration of lymphatic vessels leading to the oozing of excess lymphatic exudate, resulting from the accumulation of free radicals and reactive oxygen species (ROS). Dilated congested intertubular blood vessels and an increase in collagen fibers deposition were also detected. The thickness of the capsule in both treated groups was significantly increased compared to the control groups, and this was in agreement with the observations obtained by Awadalla and Salah-Eldin (2005) [20] and Essam Hafez et al. (2015) [21]. They investigated the hepatorenal toxicity in adult albino male rats under the tramadol effect. Moreover, Elkhateeb et al. (2015) [22] indicated that a significant decrease in glutathione peroxidase and a significant increase in hepatic and renal malondialdehydes under tramadol administration might result in oxidative stress and hepatorenal toxicity in adult albino rats.

The wide intercellular spaces noticed among spermatogenic cells may be due to apoptosis and shrinkage of the cells. These findings were similar to the results obtained by Mohamed et al. (2014) [23], who examined cadmium impact

on testicular tissues in adult male albino rats. They indicated that widening of intercellular spaces is associated with disrupting the blood-testis barrier, which allows passage of toxic agents among the cells under the effect of ROS on spermatogenic cells. Furthermore, Sertoli cells and most the spermatogenic cells showed cytoplasmic vacuolations. These changes most likely developed from endoplasmic reticulum vesiculation and dilatation as well as mitochondrial swelling. Nolte et al. (1995) [24] reported that significantly larger vacuoles are phagocytotic vacuoles that continue to remain after necrotic germ cells digestion.

Marked depletion of spermatogenic population and many spermatogenic cells are replaced by vacuoles. Focal disorganization and shrunken or atrophy of seminiferous tubules detected in the present study were consistent with the findings of Caju et al. (2011) [25] and Abdellatief et al. (2015) [17], who suggested that these changes were related to endocrine and paracrine functions disturbance through disturbing luteinizing hormone (LH), estradiol, somatotropin, somatostatin, prolactin, and gonadotrophin-releasing hormone levels acted on the hypothalamus or pituitary gland. Moreover, Ahmed and Kurkar (2014) [26] stated that tramadol causes a significant decrease in the plasma levels of LH, FSH, testosterone, and total cholesterol, whereas it causes an increase in the levels of prolactin and estradiol.

Electron microscopic examination of tramadol treated groups (Ib and IIb) showed that the basement membrane was irregular, discontinuous, and surrounded by scattered collagen fibers. The same observations were recorded by Ahmed and Kurkar (2014) [26]. They explained that oxidative stress and overproduction of nitric oxide result from a reduction of scavenger antioxidant enzymes, caused by tramadol treatment.

Many studies have explained the relationship between oxidative stress and tramadol-induced reproductive toxicity, as tramadol interacts with molecular oxygen and can initiate a cascade of reactions producing numerous free radicals, such as superoxide and hydrogen peroxide, by which induction of lipid peroxidation and reduction of antioxidant enzymes in different tissues occurred [27].

Berruti (2006) [28] stated that basement membrane thickness which is observed in this study may be related to increased glycosaminoglycans and proteoglycans production. He considered the collagen type IV in the basement membrane as a defense mechanism against free radicals' damaging activity. Moreover, Lombardo et al. (2005) [29]

reported that certain stimulants might induce myoid cells to produce more collagen and extracellular matrix, responsible for the thickening of the basal lamina. Also, decreasing the proteolysis rate in the extracellular matrix or increasing collagen production from myoid cells may be the reason for the deposition of collagen into the basement membrane [30].

In this study, sloughing of germinal epithelium and seminiferous tubules atrophy were primarily detected in the juvenile treated group. Heidari et al. (2012) [31] indicated that the effect of opioids on the pituitary or hypothalamus leads to inhibiting LH release, which causes a decrease in testosterone. Furthermore, Sorge and Stewart (2006) [32] reported that testicular metabolism impairment followed by hypoplasia of germinal cells and atrophy of tubules could occur due to increased basement membrane thickness.

Coinciding with our results, it was found that tramadol induced suppression of FSH and LH [17, 25]. This could lead to a reduction in tubular diameter and degeneration of spermatogenic cells. Consequently, this would lead to widening of the peritubular tissue and thickening in the basement membrane observed in Masson's trichrome-stained sections of the present study. This observation was in line with the results of [33], who accounted for the widening of peritubular tissue due to the withdrawal of gonadotrophic stimulation after hypophysectomy. Some authors explained germ cell sloughing because affected Sertoli cells induced a decrease in seminiferous tubule fluid secretion, which further resulted in apical sloughing or shedding and germ cell death. Others attributed the sloughing of germ cells to the organization of germ cells held in place by a close association between their membranes and specialized junctions of cell membranes of Sertoli cells [33, 34]. In the present study, ultrastructural analysis of testicular tissue revealed extensive degenerative changes in spermatogenic and Sertoli cells in some seminiferous tubules up to the complete depletion of cells. These features agreed with the findings of Jezek et al. (1993) [35]. They explained Sertoli cell vacuolation due to metabolic disturbance. It is well known that Sertoli cells are influenced mainly by testosterone, producing androgen-binding protein and other products under the control of FSH and androgens [36]. We postulated that tramadol administration disturbed this link and induced morphological alteration due to testosterone deprivation.

In this study, our result showed that tramadol triggered atrophy and apoptosis by the stimulation of apoptotic molecules via increased activation of caspase-3 in testes

which was revealed by immunohistochemistry staining, as tramadol led to the increase of the number and intensity of caspase-3 positive cells in both tramadol treated groups compared to control groups. The damage to the mitochondria may explain this. Mohamed and Mahmoud (2019) [37] reported that chronic tramadol consumption induced oxidative damage leading to inflammation, and apoptosis. This may be explained by activation and expression of the inflammation and apoptosis markers and a decrease in the anti-apoptotic proteins. Another explanation of apoptosis is the increased DNA fragmentation induced by exogenous opioids in men [38].

The sperms and spermatids were infrequently seen in the present work. This may be explained by the release of cytotoxic reactive oxygen species that cause tissue injury, especially in the late phase of differentiation of germ cells [39]. Moreover, Eddy (1999) [40] mentioned that the spermatocytes arrested in prophase meiosis were then eliminated at the late pachytene phase by apoptosis, resulting in the absence of spermatids.

Furthermore, electron microscopic examination of the testes of treated groups (Ib and IIb) showed some spermatogenic cells rupture with small dark nuclei. The same observations were detected by Newton et al. (2005) [41] and Tamura et al. (2012) [42], who said that the free radicals facilitate the release of lysosomal enzymes into cytosol with subsequent oxidation of the protein components of the cell, causing their fragmentation.

Leydig cells nuclei were irregular with dilated smooth endoplasmic reticulum and many vacuoles in the cytoplasm in both tramadol-treated groups. These findings agreed with the results obtained by Ghoneim et al. (2014) [9]. In addition, Ahmed and Kurkar (2014) [26] detected a reduction in Leydig cells numbers with their malformation. An extreme increase in testicular nitric oxide level occurred with repeated tramadol administration in rats for several weeks. These results could suggest Leydig cells' hypofunction and a decrease in testosterone production [43-45]. Recently, Bassiony et al. (2020) [46] stated that patients treated with tramadol were more likely to have lower free testosterone levels and lower sperm counts and vitality. This was accompanied by higher prolactin levels and abnormal forms of sperm compared with controls. These findings may be explained by Popovic et al. (2009) [47], who related Leydig cells degeneration to oxidative stress that generates ROS reacting with protein, nucleic acids, and lipids, causing function and structure changes

and finally damage and even death of the cells. Moreover, El-Gaafarawi (2006) [48] reported that tramadol directly affected the hypothalamic-pituitary axis inhibiting the secretion of both FSH and LH, which are responsible for normal spermatogenesis in male rats, and reduction of testosterone secretion, which could be involved in the involution of the seminiferous epithelium.

In conclusion, tramadol has a deleterious effect on testicular tissues of both juvenile and adult male albino mice, but tramadol impact was more evident in juvenile mice. Tramadol abuse, especially in the juvenile treated group, may solve the association between its use and unexplained late fertility, such as damage to testicular tissues, apoptosis, lipid peroxidation, induced oxidative stress reducing sperm production. So, tramadol abuse should be stopped and used only with a medical prescription, to avoid its harmful effect.

Attention from the Egyptian Institutes of education and health, together with families, is required to prohibit tramadol overuse, reduce its popularity, and decrease its addiction among young people.

ORCID

Amal T. Abou Elghait:
https://orcid.org/0000-0002-5173-6320
Tarek. M. Mostafa:
https://orcid.org/0000-0002-3072-2034
Fatma K. Gameaa: https://orcid.org/0000-0002-4873-4148
Gamal K. Mohammed:
https://orcid.org/0000-0001-7269-4062
Fatma Y. Meligy: https://orcid.org/0000-0002-6372-8731
Manal M. Sayed: https://orcid.org/0000-0003-0842-4548

Author Contributions

Conceptualization: ATAE, GKM. Data acquisition: FYM. Data analysis or interpretation: MMS. Drafting of the manuscript: FKG. Critical revision of the manuscript: TMM, FYM. Approval of the final version of the manuscript: all authors.

Conflicts of Interest

No potential conflict of interest relevant to this article was reported.

References

1. Candeletti S, Lopetuso G, Cannarsa R, Cavina C, Romualdi P. Effects of prolonged treatment with the opiate tramadol on prodynorphin gene expression in rat CNS. J Mol Neurosci 2006;30:341-7.

2. Hawton K, Bergen H, Simkin S, Wells C, Kapur N, Gunnell D. Six-year follow-up of impact of co-proxamol withdrawal in England and Wales on prescribing and deaths: time-series study. PLoS Med 2012;9:e1001213.

3. Miotto K, Cho AK, Khalil MA, Blanco K, Sasaki JD, Rawson R. Trends in tramadol: pharmacology, metabolism, and misuse. Anesth Analg 2017;124:44-51.

4. Leppert W, Łuczak J. The role of tramadol in cancer pain treatment--a review. Support Care Cancer 2005;13:5-17.

5. Grond S, Sablotzki A. Clinical pharmacology of tramadol. Clin Pharmacokinet 2004;43:879-923.

6. Babalonis S, Lofwall MR, Nuzzo PA, Siegel AJ, Walsh SL. Abuse liability and reinforcing efficacy of oral tramadol in humans. Drug Alcohol Depend 2013;129:116-24.

7. Scott LJ, Perry CM. Tramadol: a review of its use in perioperative pain. Drugs 2000;60:139-76.

8. Aloisi AM, Ceccarelli I, Fiorenzani P, Maddalena M, Rossi A, Tomei V, Sorda G, Danielli B, Rovini M, Cappelli A, Anzini M, Giordano A. Aromatase and 5-alpha reductase gene expression: modulation by pain and morphine treatment in male rats. Mol Pain 2010;6:69.

9. Ghoneim FM, Khalaf HA, Elsamanoudy AZ, Helaly AN. Effect of chronic usage of tramadol on motor cerebral cortex and testicular tissues of adult male albino rats and the effect of its withdrawal: histological, immunohistochemical and biochemical study. Int J Clin Exp Pathol 2014;7:7323-41.

10. Bar-Or D, Salottolo KM, Orlando A, Winkler JV; Tramadol ODT Study Group. A randomized double-blind, placebo-controlled multicenter study to evaluate the efficacy and safety of two doses of the tramadol orally disintegrating tablet for the treatment of premature ejaculation within less than 2 minutes. Eur Urol 2012;61:736-43.

11. Creasy DM. Histopathology of the male reproductive system I: techniques. Curr Protoc Toxicol 2002;Chapter 16:Unit16.3.

12. Bancroft JD, Layton C. The hematoxylins and eosin. In: Suvarna SK, Layton C, Bancroft JD, editors. Bancroft's Theory and Practice of Histological Techniques. 7th ed. Philadelphia: Churchill Livingstone of Elsevier; 2013. p.173-86.

13. Glauert AM, Lewis PR. Biological specimen preparation for transmission electron microscopy. Princeton: Princeton University Press; 2014.

14. O'Callaghan JP, Jensen KF. Enhanced expression of glial fibrillary acidic protein and the cupric silver degeneration reaction can be used as sensitive and early indicators of neurotoxicity. Neurotoxicology 1992;13:113-22.

15. Martyn-St James M, Cooper K, Kaltenthaler E, Dickinson K, Cantrell A, Wylie K, Frodsham L, Hood C. Tramadol for premature ejaculation: a systematic review and meta-analysis. BMC Urol 2015;15:6.

16. Ahmed AI, El-Dawy K, Fawzy MM, Abdallah HA, Elsaid HN, Elmesslamy WO. Retrospective review of tramadol abuse. Slov Vet Res 2018;55(Suppl 20):471-83.

17. Abdellatief RB, Elgamal DA, Mohamed EE. Effects of chronic tramadol administration on testicular tissue in rats: an experimental study. Andrologia 2015;47:674-9.

18. Cerilli LA, Kuang W, Rogers D. A practical approach to testicular biopsy interpretation for male infertility. Arch Pathol Lab Med 2010;134:1197-204.

19. Salama N, Bergh A, Damber JE. The changes in testicular vascular permeability during progression of the experimental varicocele. Eur Urol 2003;43:84-91.

20. Awadalla EA, Salah-Eldin A. Histopathological and molecular studies on tramadol mediated hepato-renal toxicity in rats. J Pharm Biol Sci 2005;10:90-102.

21. Essam Hafez M, Sahar Issa Y, Safaa Abdel Rahman M. Parenchymatous toxicity of tramadol: histopathological and biochemical study. J Alcohol Drug Depend 2015;3:225.

22. Elkhateeb A, El Khishin I, Megahed O, Mazen F. Effect of Nigella sativa Linn oil on tramadol-induced hepato- and nephrotoxicity in adult male albino rats. Toxicol Rep 2015;2:512-9.

23. Mohamed D, Saber A, Omar A, Soliman A. Effect of cadmium on the testes of adult albino rats and the ameliorating effect of zinc and vitamin E. Br J Sci 2014;11:72-95.

24. Nolte T, Harleman JH, Jahn W. Histopathology of chemically induced testicular atrophy in rats. Exp Toxicol Pathol 1995;47:267-86.

25. Caju FM, Queiroz GCD, Torres SM, Tenório BM, Júnior VAS. Opioid system manipulation during testicular development: results on sperm production and sertoli cells population. Acta Sci Biol Sci 2011;33:219-25.

26. Ahmed MA, Kurkar A. Effects of opioid (tramadol) treatment on testicular functions in adult male rats: the role of nitric oxide and oxidative stress. Clin Exp Pharmacol Physiol 2014;41:317-23.

27. Zhang YT, Zheng QS, Pan J, Zheng RL. Oxidative damage of biomolecules in mouse liver induced by morphine and protected by antioxidants. Basic Clin Pharmacol Toxicol 2004;95:53-8.

28. Berruti G. Signaling events during male germ cell differentiation: update, 2006. Front Biosci 2006;11:2144-56.

29. Lombardo F, Sgrò P, Salacone P, Gilio B, Gandini L, Dondero F, Jannini EA, Lenzi A. Androgens and fertility. J Endocrinol Invest 2005;28(3 Suppl):51-5.

30. Soliman HM, Wagih HM, Attia GM, Algaidi SA. Light and electron microscopic study on the effect of antischizophrenic drugs on the structure of seminiferous tubules of adult male albino rats. Folia Histochem Cytobiol 2014;52:335-49.

31. Heidari Z, Mahmoudzadeh-Sagheb H, Kohan F. A quantitative and qualitative study of rat testis following administration of methadone and buprenorphine. Int J High Risk Behav Addict 2012;1:14-7.

32. Sorge RE, Stewart J. The effects of long-term chronic buprenorphine treatment on the locomotor and nucleus accumbens

dopamine response to acute heroin and cocaine in rats. Pharmacol Biochem Behav 2006;84:300-5.

33. Rashed RMA, Mohamed IK, El-Alfy SH. Effects of two different doses of melatonin on the spermatogenic cells of rat testes: a light and electron microscopic study. Egypt J Histol 2010;33:819-35.

34. Manivannan B, Mittal R, Goyal S, Ansari AS, Lohiya NK. Sperm characteristics and ultrastructure of testes of rats after long-term treatment with the methanol subfraction of Carica papaya seeds. Asian J Androl 2009;11:583-99.

35. Jezek D, Simunić-Banek L, Pezerović-Panijan R. Effects of high doses of testosterone propionate and testosterone enanthate on rat seminiferous tubules--a stereological and cytological study. Arch Toxicol 1993;67:131-40.

36. Sharpe RM, McKinnell C, Kivlin C, Fisher JS. Proliferation and functional maturation of Sertoli cells, and their relevance to disorders of testis function in adulthood. Reproduction 2003;125:769-84.

37. Mohamed HM, Mahmoud AM. Chronic exposure to the opioid tramadol induces oxidative damage, inflammation and apoptosis, and alters cerebral monoamine neurotransmitters in rats. Biomed Pharmacother 2019;110:239-47.

38. Drobnis EZ, Nangia AK. Pain medications and male reproduction. Adv Exp Med Biol 2017;1034:39-57.

39. Erkkilä K, Aito H, Aalto K, Pentikäinen V, Dunkel L. Lactate inhibits germ cell apoptosis in the human testis. Mol Hum Reprod 2002;8:109-17.

40. Eddy EM. Role of heat shock protein HSP70-2 in spermatogenesis. Rev Reprod 1999;4:23-30.

41. Newton AP, Cadena SM, Rocha ME, Carnieri EG, Martinelli de Oliveira MB. Effect of triclosan (TRN) on energy-linked functions of rat liver mitochondria. Toxicol Lett 2005;160:49-59.

42. Tamura I, Kanbara Y, Saito M, Horimoto K, Satoh M, Yamamoto H, Oyama Y. Triclosan, an antibacterial agent, increases intracellular Zn(2+) concentration in rat thymocytes: its relation to oxidative stress. Chemosphere 2012;86:70-5.

43. Abdel-Zaher AO, Abdel-Rahman MS, Elwasei FM. Protective effect of Nigella sativa oil against tramadol-induced tolerance and dependence in mice: role of nitric oxide and oxidative stress. Neurotoxicology 2011;32:725-33.

44. Halawa AM. Effect of sildenafil administration on ischemic reperfusion of the testis in adult albino rat light and electron microscopic study. Egypt J Histol 2010;2:380-95.

45. Gouda ZA, Selim AO. A possible correlation between the testicular structure and short photoperiod exposure in young albino rats: light and electron microscopic study. Egypt J Histol 2013;36:28-38.

46. Bassiony MM, Youssef UM, El-Gohari H. Free testosterone and prolactin levels and sperm morphology and function among male patients with tramadol abuse: a case-control study. J Clin Psychopharmacol 2020;40:405-8.

47. Popovic M, Janicijevic-Hudomal S, Kaurinovic B, Rasic J, Trivic S, Vojnović M. Antioxidant effects of some drugs on immobilization stress combined with cold restraint stress. Molecules 2009;14:4505-16.

48. El-Gaafarawi II. Biochemical toxicity induced by tramadol administration in male rats. Egypt J Hosp Med 2006;23:353-62.